

Original Article

GDF15 negatively regulates RGS16 to impair hepatic lipid metabolism in male mice offspring conceived by in vitro fertilization

Jingliu Liu^{1*}, Yichen Zhu^{2*}, Dan Zhu¹, Yajun Shi¹, Likui Lu¹, Weisheng Li¹, Lingjun Li¹, Xiuwen Zhou¹, Pengjie Zhang¹, Hao Yang¹, Min Li³, Bin Wang¹, Miao Sun¹

¹Institute for Fetology, The First Affiliated Hospital of Soochow University, Suzhou, Jiangsu, China; ²Cambridge-Suda Genomic Resource Center, Jiangsu Key Laboratory of Neuropsychiatric Diseases Research, Suzhou Medical College of Soochow University, Suzhou, Jiangsu, China; ³Department of Obstetrics and Gynecology, The First Affiliated Hospital of Soochow University, Suzhou, Jiangsu, China. *Equal contributors.

Received June 27, 2022; Accepted September 29, 2022; Epub October 15, 2022; Published October 30, 2022

Abstract: Objectives: We generated an in vitro fertilization and embryo transfer (IVF-ET) mouse model to investigate the molecular mechanism underlying the abnormal lipid metabolism found in IVF-ET offspring. Methods: The glucose metabolism levels of offspring were assessed by glucose tolerance test (GTT), insulin tolerance test (ITT), and pyruvate tolerance test (PTT). The lipid metabolism levels were assessed by triglycerides (TG), low-density lipoprotein cholesterol (LDL-C) and high-density lipoprotein cholesterol (HDL-C). RNA-seq was performed on liver tissues. mRNA and protein expression of relevant genes was verified by the quantitative real-time PCR and protein immunoblotting. HepG2 cells were transfected with either interfering RNA or overexpression plasmids to investigate the gene functions. Results: Compared to the control, male IVF-ET offspring showed: 1) higher body, liver, and epididymal white adipose tissue weight; 2) disrupted glucolipid metabolism with abnormal GTT, ITT, and PTT; 3) significantly decreased GDF15 along with increased RGS16. Furthermore, phosphorylation of ERK1/2 and AKT was significantly reduced. In HepG2 cells, knockdown of GDF15 caused an abnormally increased RGS16 and decreased phosphorylation of ERK1/2 and AKT, accompanied by increased lipid deposition. In contrast, overexpression of GDF15 reduced expression of RGS16. Simultaneous knockdown of both GDF15 and RGS16 reversed lipid deposition. Conclusions: Down-regulation of GDF15 results in elevated RGS16, which causes the weakening of the downstream ERK1/2 and AKT phosphorylation, leading to abnormal lipid metabolism in the livers of IVF-ET male offspring. This suggests that the GDF15-RGS16-p-ERK1/2/p-AKT pathway plays a crucial role in liver lipid deposition in IVF-ET male offspring and could be a therapeutic target.

Keywords: In vitro fertilization-embryo transfer, liver, lipid deposition, GDF15, RGS16

Introduction

Assisted reproductive technology (ART) refers to medical aids that enable infertile couples to conceive. It includes in vitro fertilization and embryo transfer (IVF-ET) and their derivatives [1]. In recent years, the incidence of infertility has increased, and about 17% of couples worldwide suffer from infertility [2]. In China, about 200 thousand IVF babies are born each year. Especially with the unveiled “three-child” policies, in order to resolve fertility problems, the demands for ART have increased dramatically. Consequently, the proportion of children born after IVF keeps rising.

Theories of “gamete and embryo-fetal origins of adult diseases” suggest that adverse environmental exposures during gametogenesis, embryo implantation, and critical developmental stages from fetus to the infant will have an “imprinting” impact on the offspring’s growth and development, leading to greater risk of diseases such as hypertension, diabetes, kidney disease, and centripetal obesity in adulthood [3]. As one of the environmental exposures at early developmental stages, ARTs involve ovarian stimulation, in vitro fertilization or intracytoplasmic single sperm injection, and embryo culture, freezing, and transfer, all of which mean that the environment experienced by gametes

Impact of IVF-ET technology on hepatic lipid metabolism of offspring

and embryos is significantly altered compared to natural pregnancy [4, 5].

Whether ARTs affect children's health in the long term has been a topic of great interest since the first IVF baby was born in 1978 [6]. A follow-up study shows that IVF-ET-born children may have a higher risk of cardiometabolic disease [7]. Increased fasting blood glucose levels [8], blood pressure [8, 9], adiposity, triglyceride levels [10], and vascular dysfunction [9, 11, 12] were found in IVF children. Our recent studies reported that umbilical veins of IVF-ET offspring showed abnormal sensitivity to acetylcholine (ACh) or angiotensin II (All)-mediated contraction, which could be caused by hypo/hypermethylation of the specific receptors [13, 14]. Our findings strongly supported the idea that IVF-ET could directly affect fetal vessel functions, which might result in cardiovascular disorders in the long term.

However, various causes of infertility and complicated genetic backgrounds in humans make the studies exploring the influence of ART itself on offspring health quite tricky. To eliminate those complicating factors, animal models were used to study the potential effects of IVF-ET on their offspring. Recent research with IVF-ET mouse models found impaired metabolism in IVF-ET offspring, such as altered fasting blood glucose levels, impaired glucose tolerance and pyruvate [15-19]; increased body weight, body fat, and higher triglyceride, cholesterol, and insulin levels [20]; decreased lipolysis and increased accumulation of lipids in adipose and liver tissues [19, 21]. These studies suggest that the IVF-ET technique is significantly associated with abnormal metabolic function in the offspring.

Abnormal glucose metabolism and its underlying mechanism have been widely investigated with ART offspring, while the altered lipid metabolism in IVF-ET offspring is seldom studied. Therefore, we generated a C57BL/6N mouse model by IVF-ET technology to study the liver function and lipid metabolism of IVF-ET-2 cell offspring and then explored the correlation between IVF-ET technology and the alteration of metabolic function of offspring and the specific mechanism.

Materials and methods

Animals

Procedures for the experiments on mice were approved by the Jiangsu Model Organisms Center's Ethical Committee. C57BL/6N mice and ICR mice were kept in a chamber with alternating light and dark, constant temperature and humidity, and no specific pathogens throughout the experiment. Pregnant mice were housed in a single cage, and pups were sorted into separate cages four weeks after birth. Mice that need to be measured for food intake are housed in a single cage.

The design of the main experiment for this study was shown in **Figure 1A**. Mice from the IVF-ET group were obtained by transferring 2-cell stage embryos (C57BL/6N background) that developed in vitro into the oviducts of pseudopregnant ICR mice. Control group (CON) refers to animals conceived naturally. Newborn pups were weighed. Offspring were individually weighed from 4 to 28 weeks after weaning. Daily food intake was assessed with both groups.

In vitro fertilization

Superovulation was performed in 6-10-week-old female C57BL/6N mice by injection of 5 IU of pregnant horse serum gonadotropin (PMSG) and 5 IU of human chorionic gonadotropin (HCG, Ningbo Second Hormone Factory, China). Oocytes and capacitated sperm were co-cultured in human oviductal fluid medium (HTF, Sigma, USA) in a 5% CO₂ and 5% O₂ incubator (Heal Force, Shanghai, China) at 37°C. After 15 h, 2-cell embryos were washed with Potassium simplex optimized medium (KSOM, Sigma, USA) three times, followed by embryo transfer.

Embryo transfer

6-8-week-old female ICR mice were used as recipient mice which were mated with male ICR mice with vasectomized vas deferens. The day when the plugs were observed was considered to be embryonic day 0.5 (E0.5) of the pseudopregnancy. Mice were anesthetized with tribromoethanol and fresh 2-cell embryos were transferred by surgery into the oviducts of pseudopregnant ICR females. All female mice that received embryos were fed standard chow and water.

Impact of IVF-ET technology on hepatic lipid metabolism of offspring

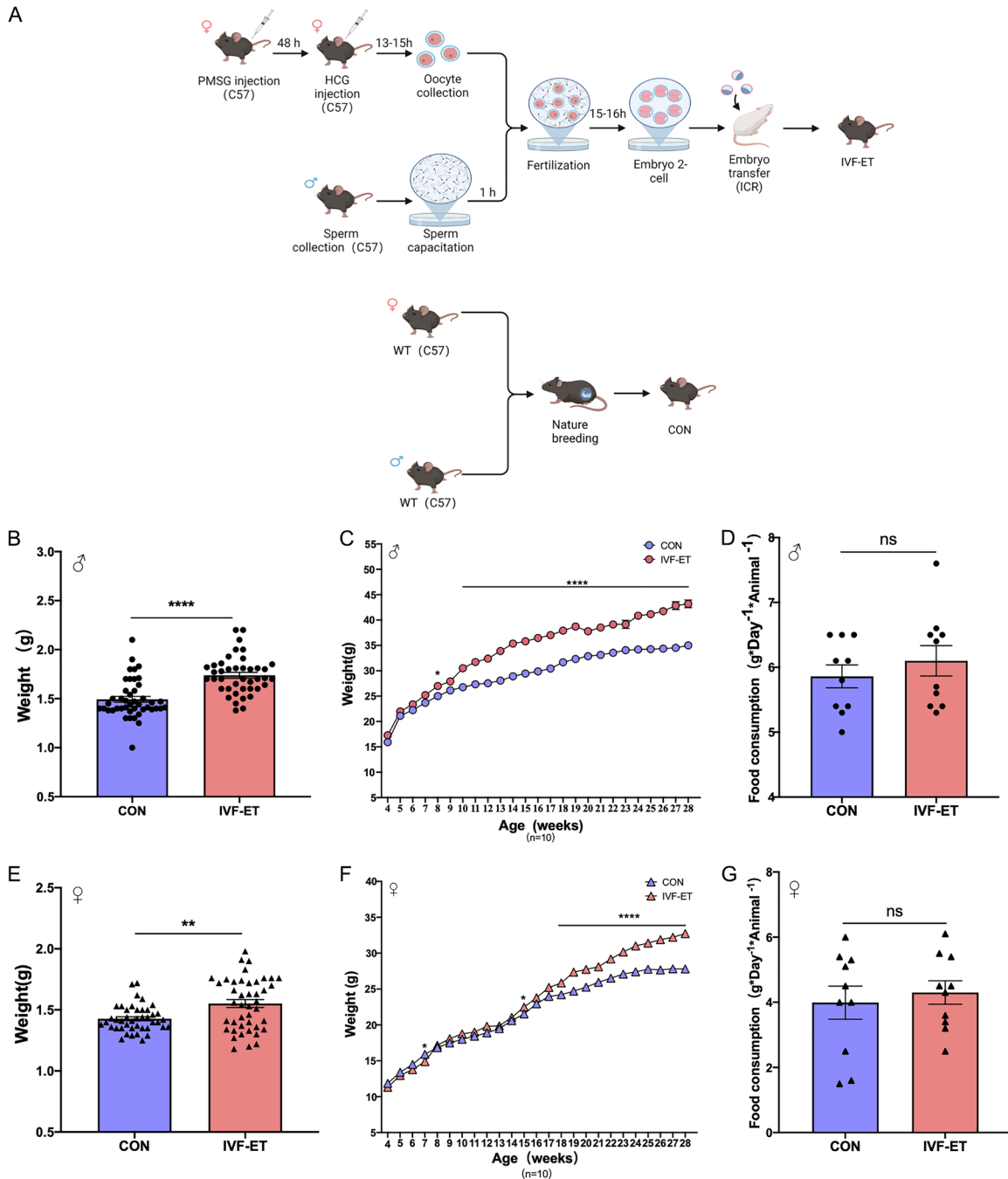


Figure 1. Experimental design, birth weights, growth charts, and food intake of offspring. (A) Experimental design (Created with Biorender.com). (B) Birthweights of male offspring (CON: n=44; IVF-ET: n=42). (C) Male offspring growth curve after weaning (CON: n=10; IVF-ET: n=10). (D) Food intake in male offspring (CON: n=10; IVF-ET: n=10). (E) Birthweights of female offspring (CON: n=43; IVF-ET: n=43). (F) Female offspring growth curve after weaning (CON: n=10; IVF-ET: n=10). (G) Food intake in female offspring (CON: n=10; IVF-ET: n=10). Data are expressed as mean ± SEM. Symbols under curves: ♂, male; ♀, female; **, $P < 0.01$; ****, $P < 0.0001$; ns, not significant. Significance was determined by 2-tailed unpaired t-test in (B, D, E, and G), and 2-way ANOVA in (C and F).

Glucose, insulin, and pyruvate tolerance test

At 20-24 weeks, mice were treated with intraperitoneal injection of glucose (2 g/kg) or pyru-

vate solution (2 g/kg) after 14-16 hours of fasting and challenged with intraperitoneal injection of insulin (1 IU/kg) after 2 hours of fasting. Blood was taken from the tail tip. Glucose lev-

Impact of IVF-ET technology on hepatic lipid metabolism of offspring

els were assessed by glucometer (Johnson, America) measurements at 0, 15, 30, 60, 90, and 120 min after injection.

Lipid values

After 4 hours of fasting, blood was collected from the posterior orbits of anesthetized mice to extract serum and stored at -80°C . Liver lipids were isolated from liver tissue. Triglycerides (TG), low-density lipoprotein cholesterol (LDL-C) and high-density lipoprotein cholesterol (HDL-C) were measured all measured with a biochemical analyzer (BMG, Germany).

Histologic analysis Liver tissues were obtained from mice at 20 weeks old after a 4-hour fast. Tissues were either fixed in 4% paraformaldehyde for hematoxylin-eosin (H&E) staining and oil red staining or frozen in liquid nitrogen for future use. All sections were visualized by microscopy (Olympus, Japan).

RNA-sequencing (RNA-seq)

Total RNA was isolated from livers using TRIzol (Invitrogen, USA). RNA sequencing was performed with the liver samples from 20-week-old male offspring. Sequencing was performed on Azenta Biotechnology's Illumina system (Soochow, China). Differentially expressed genes (DEGs) were identified by $|\text{foldchange}| > 1$ and P values < 0.05 . Volcano map, heat map and Gene set enrichment analysis (GSEA) were performed. Images are plotted on the omicstudio Biology (website: <https://www.omicstudio.cn/index>). The genes enriched in GSEA were considered significant when $P < 0.05$ and $|\text{NES}| > 1$.

Quantitative real-time PCR (qRT-PCR)

Total RNA was extracted using TRIzol (Invitrogen, USA) and synthesized cDNA with a reverse transcription kit (Thermo Scientific, USA). The TB green (TaKaRa, USA) was used for RT-qPCR. Real-time PCR was performed on Bio-Rad CFX96 RT-qPCR machine. RNA concentration and quality were analyzed using NanoDrop-2000. Gene expression was normalized to 18S or β -Actin. See [Supplementary Table 1](#) for primers.

Western blotting

Total proteins from cells and liver tissue were extracted in RIPA buffer (P0013B, Beyotime, China). After separation by gel electrophoresis,

the proteins were transferred to a nitrocellulose filter membrane. See [Supplementary Table 2](#) for antibodies. The signals were visualized with an enhanced Chemiluminescent (NCM Biotech, China) and quantified with ImageJ.

Cell culture and transfection

HepG2 cells were purchased from ATCC and were cultured in medium containing 10% fetal bovine serum (Hyclone, Logan, USA) and 1% antibiotics (Hyclone, Logan, USA). Transfection was performed using 150 pmol of si-NC, si-GDF15, si-RGS16 (Gene Pharma, Shanghai, China) or 2 μg pcDNA-empty, pcDNA-GDF15. GT-Transfect-Mate reagent (Gene Pharma, Shanghai, China) in Opti-MEM (Thermo Fisher Scientific, USA) was used. See [Supplementary Table 3](#) for siRNA information. The forward oligonucleotide sequence of the pcDNA-GDF15 vector is TAATACGACTCACTATAGGGCCACCATGCCC GGCAAGA AACTCAG; and the reverse oligonucleotide is TCTGAGATGAGTTTTTGTCTATGCAGTGGCAGTCTTTGGCT.

Oil red staining of HepG2 cells

Lipid droplets were quantified by oil red O (ORO) staining (Solarbio, Beijing, China). After transfection for 48 h, the cells were fixed in 4% paraformaldehyde and then were stained with ORO solution, the red stained lipid droplets were visualized by microscopy. TG content in HepG2 cells was measured with the Triglyceride Quantification Kit (Jiancheng, Nanjing, China).

Statistical analysis

All data are shown as mean \pm SEM. Statistical analyses were performed using GraphPad Prism 9.0 with a t-test or two-way analysis of variance (ANOVA). P -values < 0.05 were considered significant.

Results

Distinct body weight trajectories in offspring

The number of litters was similar in both groups (CON: 161, IVF-ET: 133), and the sex ratio (female/male) was 1.1 (84:77) in the CON group and 1.0 (67:66) in the IVF group (**Table 1**). The birth weights of both male and female offspring in the IVF-ET group were higher than those in the CON group on postnatal day 1 (**Figure 1B, 1E**). There was no significant differ-

Impact of IVF-ET technology on hepatic lipid metabolism of offspring

Table 1. Litter characteristics of offspring

| Group | Pregnancy rate (%) | Implantation rate (%) | Litter (n) | Pups (n) | Litter Size (n) | Sex Ratio (% F/M) | Survival Rate (%) |
|--------|--------------------|-----------------------|------------|----------|-----------------|-------------------|-------------------|
| CON | / | / | 25 | 161 | 6.4±0.4 | 1.1 (84/77) | 100 (161/161) |
| IVF-ET | 80 (20/25) | 32.2 (133/412) | 20 | 133 | 6.6±0.7 | 1.0 (67/66) | 100 (133/133) |

Data are presented as mean ± SEM; Pregnancy rate: the number of pregnant recipient mice/the number of all recipient mice; Implantation rate: the number of live pups/the number of transferred embryos; F/M: female/male. Survival Rate: the number of survival mice after weaning/the number of all born mice.

ence in body weight at four weeks; however, the weights of male IVF-ET offspring showed an upward trend at eight weeks. At ten weeks, the body weight of male mice significantly increased as compared with CON, while female offspring did not gain weight rapidly until 18 weeks (**Figure 1C, 1F**). To exclude nutritional effects, the daily intakes of the two groups were calculated, and no significant differences were observed between the IVF-ET and CON groups (**Figure 1D, 1G**). These findings showed that the IVF-ET procedure affects the development of offspring in mice.

Abnormal glucose metabolism in IVF-ET offspring

We then performed the GTT, ITT, and PTT in male and female offspring of the IVF-ET and CON groups. For the male offspring, the area under the curve (AUC) of GTT, ITT, and PTT was increased in the IVF-ET group (**Figure 2A, 2C**). Glucose homeostasis was disturbed in the IVF-ET group at 15, 30, and 90 minutes after glucose injection compared to the CON group (**Figure 2A**). ITT results showed higher blood glucose in the IVF-ET group at 0, 15, 30, and 60 minutes, indicating decreased insulin sensitivity (**Figure 2B**). Despite slight differences in fasting blood glucose, no remarkable difference in blood glucose levels in the two groups after pyruvate injection (**Figure 2C**). However, for the female offspring, there were no significant differences in fasting glucose, GTT and PTT tests between the two groups, as was the area under their curves (**Figure 2D, 2F**), and the ITT test showed differences in blood glucose at 0 and 15 minutes after insulin injection and a higher AUC in the IVF-ET group than in the CON group (**Figure 2E**), suggesting slight insulin resistance.

Abnormal lipid metabolism in IVF-ET male offspring

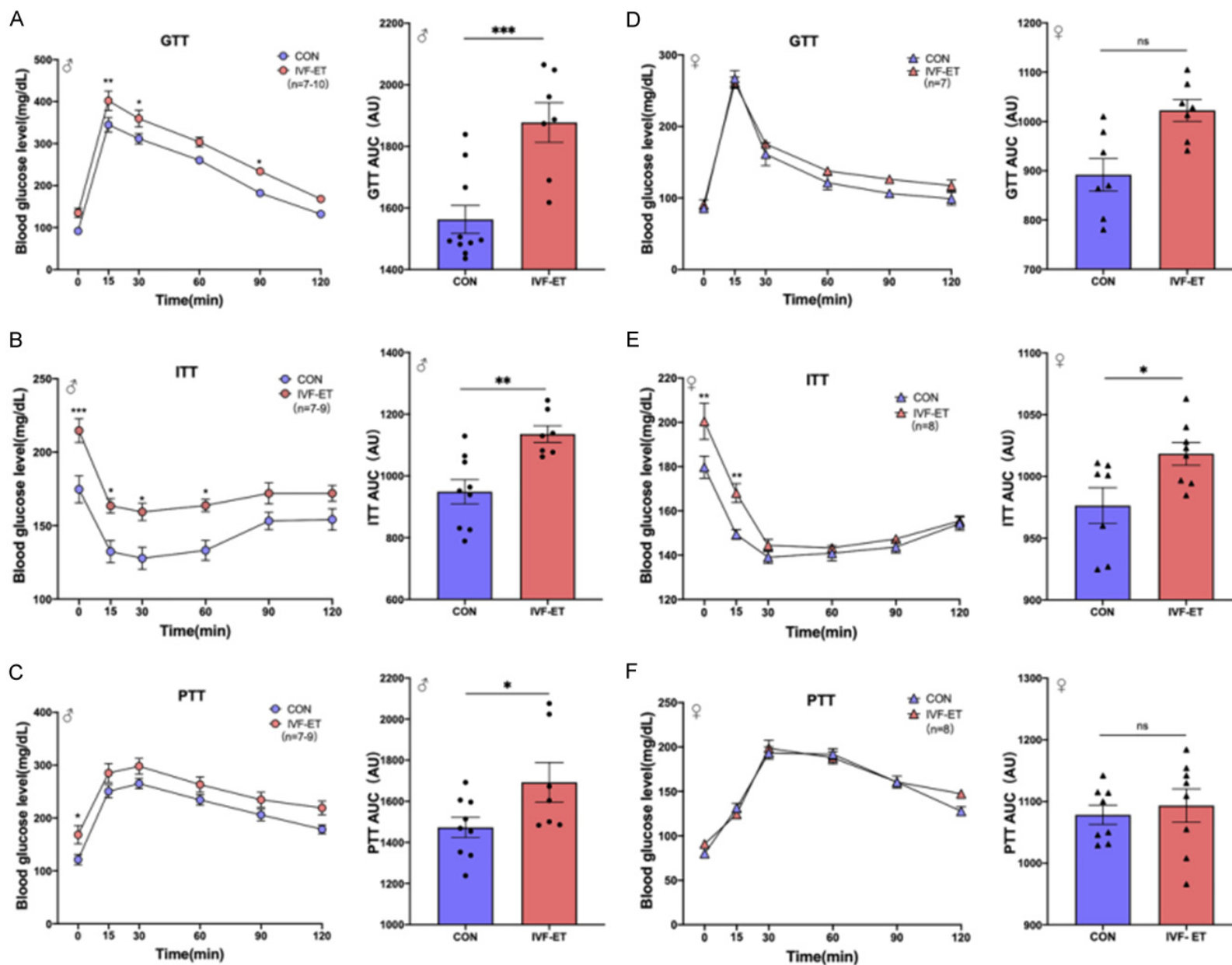
In combination with body weight data and metabolism phenotypes, IVF-ET male offspring

had more severe glucose metabolism impairment than female offspring. Therefore, male offspring were chosen as the main subjects in this study. We measured the weight of organs relevant to metabolism, such as the liver, brain, spleen, heart, kidney, subcutaneous white adipose tissue (sWAT), epididymal white adipose tissue (eWAT), and interscapular brown adipose tissue (iBAT) and calculated organ weight/body weight ratios. Both liver and eWAT weight were found to be increased, while only the ratio of epididymal fat weight/body weight, but not liver, was significantly increased (**Figure 3B, 3C**). The liver is a crucial organ in the regulation of glucose and lipid metabolism [22, 23]. H&E staining of the liver showed that the IVF-ET male offspring had extensive steatosis, ballooning degeneration, and a scattered infiltration of a small number of inflammatory cells in the hepatocytes compared to controls (**Figure 3A**). ORO staining showed significant lipid deposition in IVF-ET male offspring liver tissue (**Figure 3A**). Lipid metabolism analysis using plasma and liver tissue showed significantly increased plasma triglycerides and LDL-C and decreased HDL-C in the IVF-ET male offspring (**Figure 3D-F**). Similarly, significant increases in triglycerides and LDL-C, and decreases in HDL-C were found in the liver tissue of IVF-ET male offspring (**Figure 3G-I**). However, in the liver tissue and serum of female mice offspring, a slight increase in TG (**Supplementary Figure 1A, 1D**) and no significant differences in LDL-C and HDL-C (**Supplementary Figure 1B, 1C, 1E, 1F**) were found in the IVF-ET group compared to CON. It can be inferred that the offspring of IVF-ET males have abnormal lipid metabolism.

Altered liver transcriptome in IVF-ET male offspring

RNA sequencing of livers from both groups was performed to explore potential mechanisms of lipid metabolism in male offspring conceived through IVF-ET. 59 genes were upregulated, and 76 genes were downregulated in the IVF-

Impact of IVF-ET technology on hepatic lipid metabolism of offspring



Impact of IVF-ET technology on hepatic lipid metabolism of offspring

Figure 2. GTT, ITT, and PTT in offspring. A. Glucose tolerance test and AUC in male offspring (CON: n=10; VF-ET: n=7). B. Insulin tolerance test and AUC in male offspring (CON: n=9; IVF-ET: n=7). C. Pyruvate tolerance test and AUC in male offspring (CON: n=9; IVF-ET: n=7). D. Glucose tolerance test and AUC in female offspring (CON: n=7; VF-ET: n=7). E. Insulin tolerance test and AUC in female offspring (CON: n=8; IVF-ET: n=8). F. Pyruvate tolerance test and AUC in female offspring (CON: n=8; IVF-ET: n=8). For bar graphs, data represent mean \pm SEM. δ , male; ♀ , female; *, $P < 0.05$; **, $P < 0.01$; ***, $P < 0.001$; ns, not significant. Relative to controls, by ANOVA.

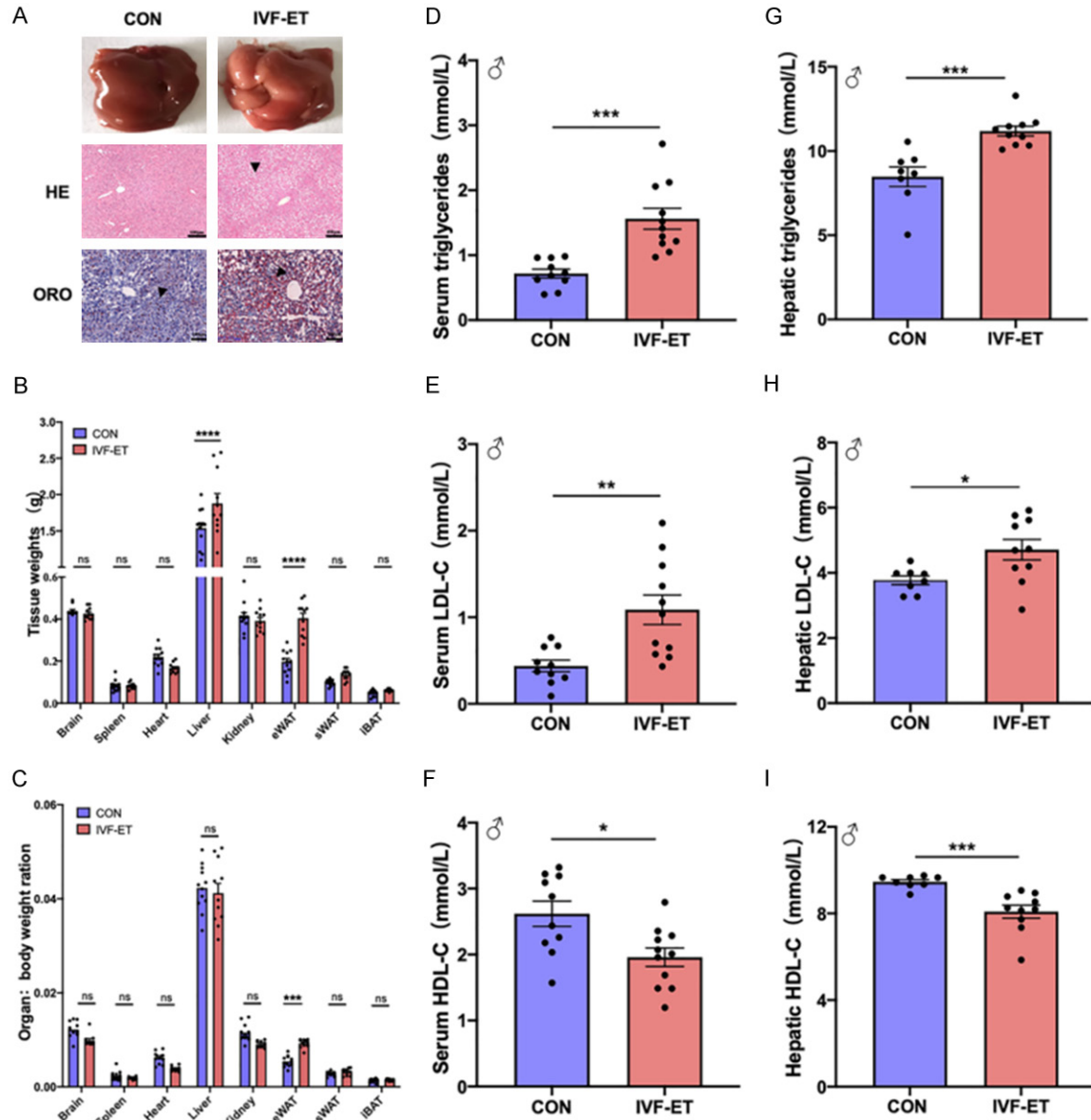


Figure 3. Analysis of liver and lipid metabolism factors in male offspring. A. H&E staining and oil-red O staining of liver tissue (scale bar =100 μm). B. Weight of multiple organs of male offspring (CON: n=12; IVF-ET: n=11). C. The proportion of each organ to body weight (CON: n=12; IVF-ET: n=11). D-F. Plasma levels of triglycerides, LDL-C, HDL-C (CON: n=10; IVF-ET: n=11). G-I. Triglycerides, LDL-C, HDL-C levels in liver tissue (CON: n=8; IVF-ET: n=10). TG, Triacylglycerol; HDL-C, High-Density Lipoprotein Cholesterol; LDL-C, Low-Density Lipoprotein Cholesterol. Data represent mean \pm SEM. *, $P < 0.05$; **, $P < 0.01$; ***, $P < 0.001$; ****, $P < 0.0001$; ns, not significant.

ET group compared to the CON group (Figure 4A). A heat map of metabolism-related genes

was generated (Figure 4B). By analyzing the GSEA it was found that many genes involved in

Impact of IVF-ET technology on hepatic lipid metabolism of offspring

the initial fatty acid synthesis process were significantly upregulated in the GO and KEGG enrichment pathways in the IVF-ET group compared to the CON group (Figure 4C, 4D). We verified the sequencing results by RT-qPCR and confirmed the upregulation of many genes related to lipid synthesis, such as *Pparg*, *Srebf1*, *Dgat2*, *Cebpb*, and *Fabp2* (Figure 4E). No significant changes were observed for several genes related to fatty acid oxidation, such as *Ppara*, *Pgc1a*, and *Acox1* (Figure 4F). Liver transcriptome data has suggested that abnormal liver lipid metabolism in IVF-ET male offspring mice may be primarily related to the lipid synthesis pathway.

Decreased GDF15 and increased RGS16 were found in the liver of IVF-ET offspring

Gdf15 performs a vital role in obesity and metabolic diseases [24, 25]. *Rgs16* was known to regulate fatty acid oxidation in hepatocytes [26]. Both of which are implicated in hepatic lipid metabolism. In RNA-sequencing results, more than 2-fold changes were found with both *Gdf15* and *Rgs16* in the IVF-ET group as compared to the CON group (Figure 4A, 4B). Validation of the expression of these two genes in mouse liver tissue by q-PCR revealed reduced *Gdf15* (Figure 5A) and increased *Rgs16* (Figure 5B), which is consistent with the results of the RNA-Seq data. Western blotting results confirmed decreased GDF15 and increased RGS16 protein expression in the livers of IVF-ET offspring (Figure 5C).

Increased phosphorylation of AKT and ERK1/2 in the livers of IVF-ET offspring

It is known that GDF15 can activate the downstream AKT and ERK1/2 pathways, which contribute to the regulation of hepatic mitochondrial function and energy metabolism. Therefore, we continued to check if the downstream of GDF15 had been affected. We verified the expression of ERK1/2, AKT, p-ERK1/2, and p-AKT levels in the liver of IVF-ET male offspring by western blot and found that the expression of p-ERK1/2 and p-AKT was reduced in the liver of IVF-ET male offspring mice (Figure 5D). This suggests that the impaired lipid metabolism in the IVF-ET group may be due to abnormalities in the ERK1/2 and AKT pathways.

GDF15 negatively regulated RGS16 in lipid deposition in hepatocytes

To investigate the relationship between GDF15, RGS16, and liver lipid metabolism, we performed RNA interference to knock down GDF15 expression in HepG2 cells in vitro. Interestingly, we found that knockdown of GDF15 was followed by an increase in the expression of RGS16 (Figure 6A, 6B). De novo lipid synthesis genes such as *PPARG*, *SREBF1*, *FABP2*, *CEBPB*, and *FABP2* were increased (Figure 6D), while fatty acid oxidation genes such as *Ppara*, *Pgc1a*, *Acox1* showed no significance (Figure 6E). Phosphorylation of ERK1/2 and AKT levels were significantly decreased (Figure 6C). Furthermore, we overexpressed GDF15 by transfecting HepG2 cells with GDF15 containing pcDNA3.1-myc-His plasmids. Interestingly, we found that overexpression of GDF15 was followed by a significant decrease in RGS16 mRNA and protein expression (Figure 7A, 7B). The expression of lipogenic genes *SREBF1* and *FABP2* was decreased (Figure 7D), while the expression of fatty acid oxidation genes *PPARA* and *ACOX1* was increased (Figure 7E). Phosphorylation of ERK1/2 and AKT were significantly increased (Figure 7C). Our findings indicated that a negative regulatory relationship between GDF15 and RGS16 may cause changes in lipogenic and fatty acid oxidation genes by affecting the phosphorylation of ERK1/2 and AKT, leading to increased lipid deposition.

Knockdown of RGS16 reverses GDF15 down-regulation-induced lipid deposition

Since decreased GDF15 results in abnormal lipid metabolism and increased expression of RGS16, we asked whether reducing RGS16 could rescue the phenotypes caused by GDF15 down-regulation.

By RGS16 RNAi in HepG2 cells (Supplementary Figure 2A, 2B), we found that RGS16 knockdown in HepG2 cells reduced expression of lipogenic genes *PPARG*, *SREBF1*, and *FABP2* mRNA (Supplementary Figure 2D), increased expression of fatty acid oxidation gene *PGC1A* (Supplementary Figure 2E) and increased phosphorylation of ERK1/2 and AKT (Supplementary Figure 2C), suggesting that a reduction in RGS16 may increase fatty acid oxidation and

Impact of IVF-ET technology on hepatic lipid metabolism of offspring

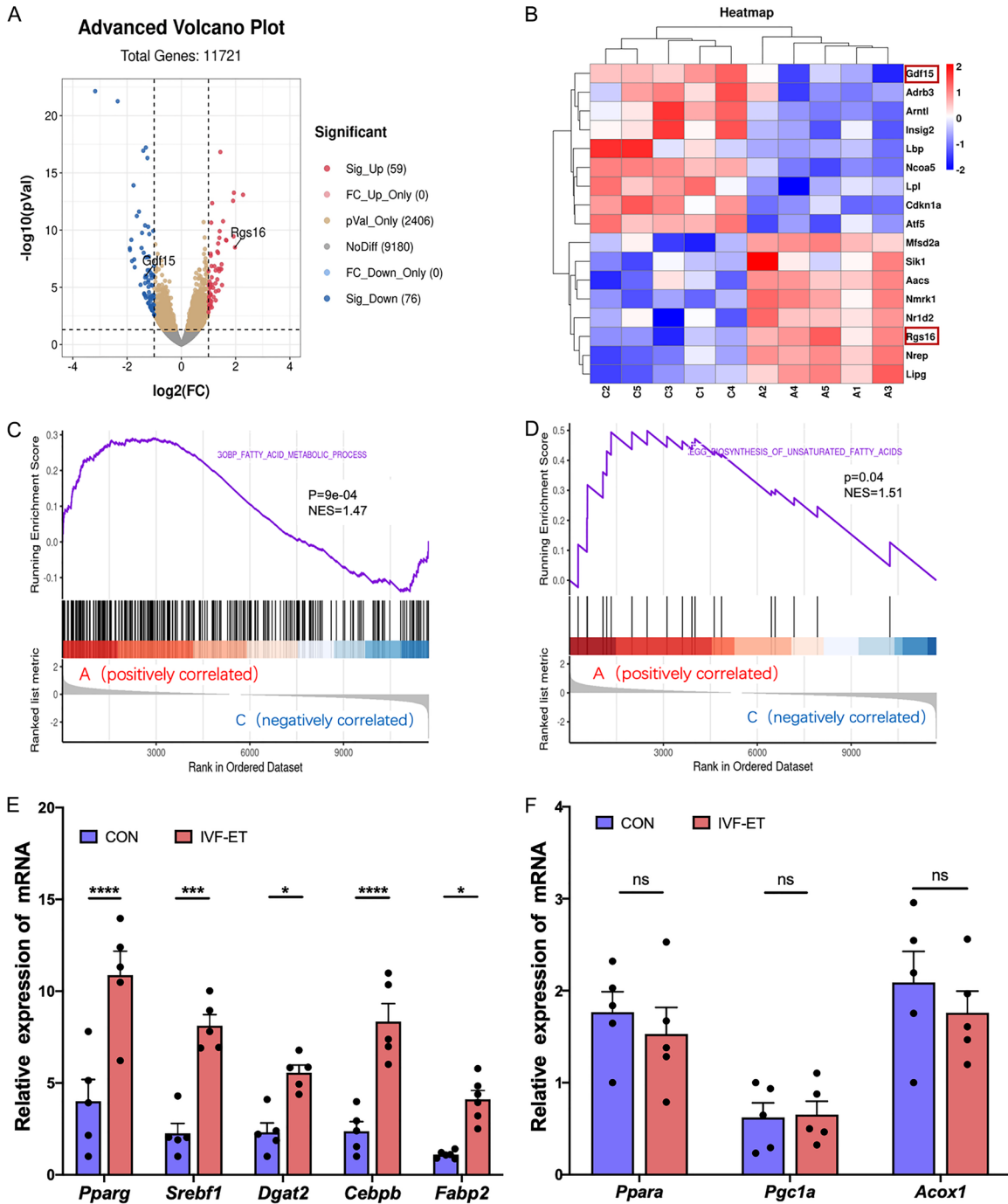


Figure 4. Transcriptome analysis in livers of IVF-ET male offspring. A. Volcano plots show significantly altered genes. *Rgs16* and *Gdf15* are highlighted; B. Heat map of differential genes associated with lipid metabolism; C. Enrichment map of genes involved in pathways related to fatty acid metabolism; D. Enrichment map of genes involved in pathways related to unsaturated fatty acid metabolism. E. mRNA levels of genes related to the fatty acid synthesis pathway in liver tissue; F. mRNA levels of genes related to the fatty acid oxidation pathway in liver tissue. GSEA, Gene Set Enrichment Analysis; NES, Normalized Enrichment Score; GO, Gene Ontology; BP, Biological Process; KEGG, Kyoto Encyclopedia Of Genes And Genomes. For bar graphs, data represent mean \pm SEM. *, $P < 0.05$; ***, $P < 0.001$; ****, $P < 0.0001$; ns, not significant.

inhibit initial lipid synthesis, resulting in reduced lipid deposition in hepatocytes.

We then knocked down of GDF15 and RGS16 expression simultaneously to see if this could

Impact of IVF-ET technology on hepatic lipid metabolism of offspring

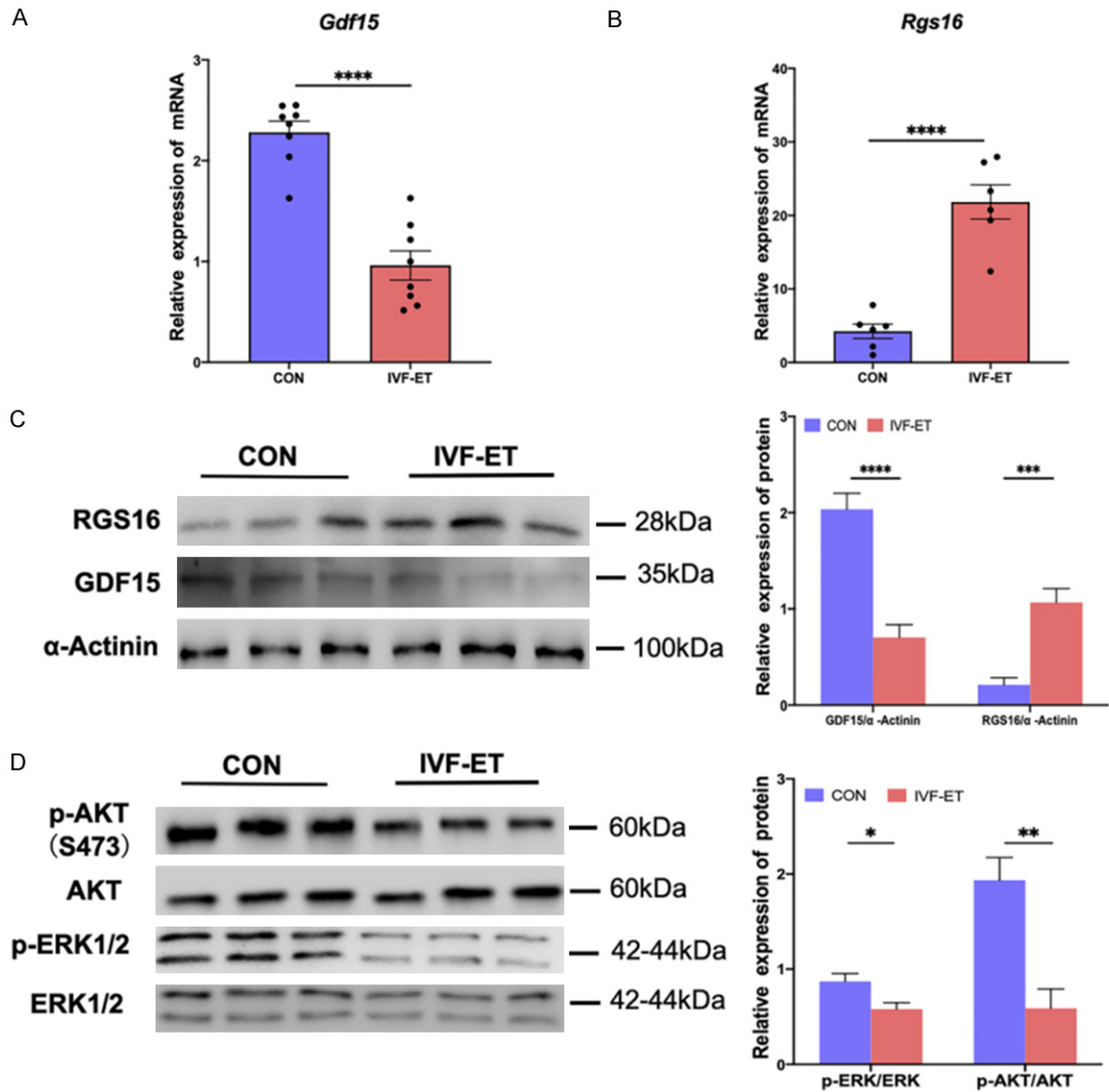


Figure 5. Expression of GDF15, RGS16, ERK1/2, AKT, and p-AKT. A. Expression levels of *Gdf15* mRNA in liver tissues of two groups of mice (CON: n=6; IVF-ET: n=6); B. Expression levels of *Rgs16* mRNA in liver tissues of mice in both groups (CON: n=6; IVF-ET: n=6); C. Protein expression of GDF15 and RGS16 in liver tissues of both groups (CON: n=5-6; IVF-ET: n=5-6); D. Protein expression of AKT, ERK1/2, p-ERK, p-AKT in liver tissues of both groups (CON: n=5-6; IVF-ET: n=5-6). For bar graphs, data represent mean \pm SEM. *, $P < 0.05$; **, $P < 0.01$; ***, $P < 0.001$; ****, $P < 0.0001$.

reverse the abnormal lipid deposition caused by GDF15 downregulation in hepatocytes. Oil Red O staining showed that knockdown of RGS16 reversed the abnormal lipid deposition (Figure 8A), mRNA expression of lipogenic and fatty acid oxidation genes (Figure 8C, 8D), and phosphorylation of ERK1/2 and AKT caused by GDF15 knockdown in HepG2 cell line (Figure 8B). These results suggested that the knockdown of RGS16 in HepG2 cells reversed the abnormal lipid deposition induced by GDF15 knockdown.

Discussion

The development of the embryo and fetus are susceptible to environmental factors, and any sub-optimal conditions during the development stages of the gametes, embryos, and fetus can affect the health of the offspring after birth, which is known as the "Gamete and embryofetal origin of disease" theory [27]. A vast body of evidence suggests that children conceived by IVF-ET may be at increased risk of chronic diseases [8, 10]. In this study, increased body

Impact of IVF-ET technology on hepatic lipid metabolism of offspring

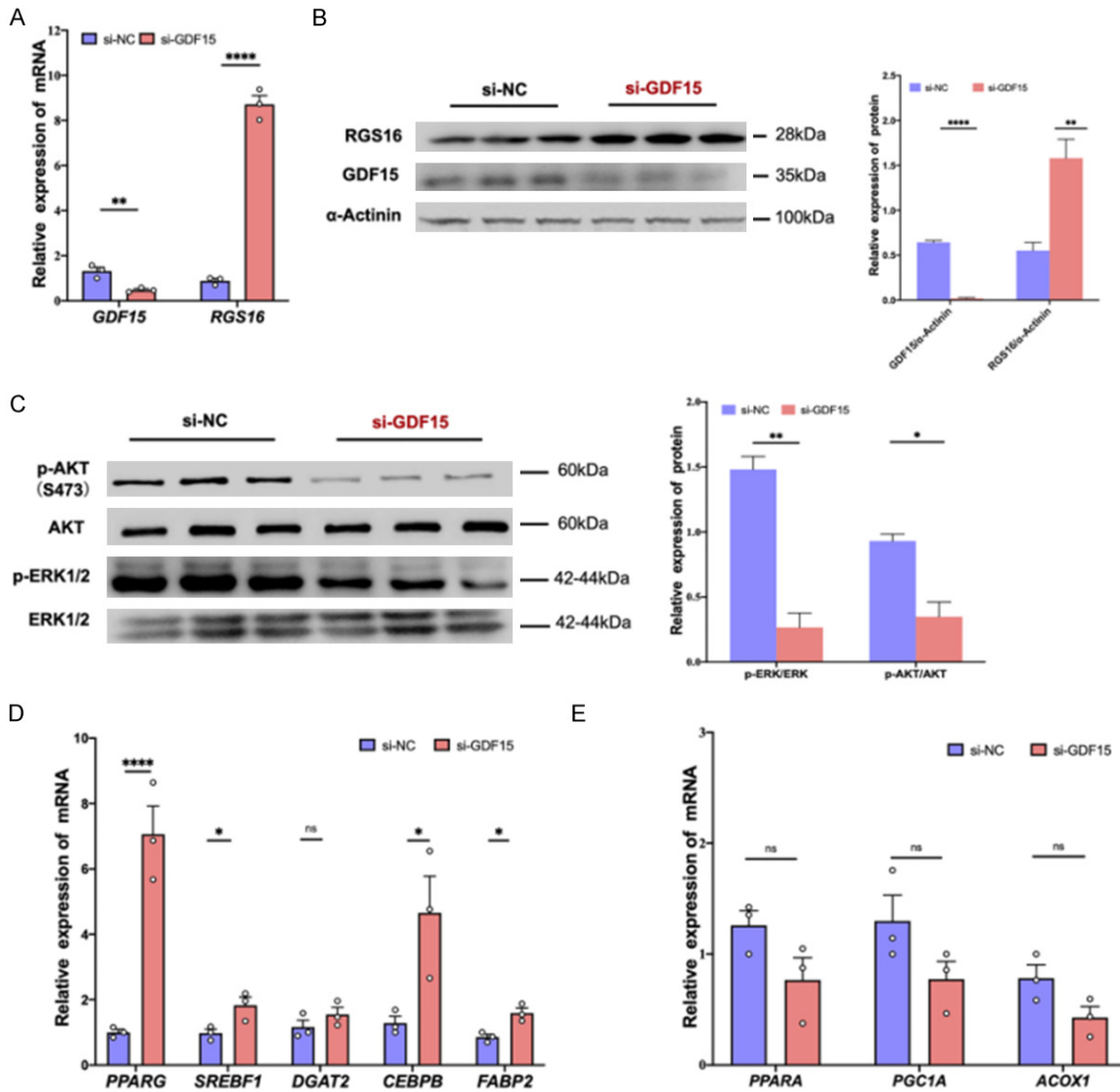


Figure 6. Relationship of GDF15 with lipid metabolism and RGS16. A. GDF15 and RGS16 mRNA expression levels after GDF15 knockout (si-NC: n=3; si-GDF15: n=3); B. Protein levels of GDF15 and RGS16 after GDF15 knockdown (si-NC: n=3-6; si-GDF15: n=3-6); C. Protein levels of AKT, ERK1/2, p-ERK1/2, p-AKT after GDF15 knockdown (si-NC: n=3-6; si-GDF15: n=3-6); D. mRNA expression levels of lipogenic genes after GDF15 knockdown (si-NC: n=3; si-GDF15: n=3); E. mRNA expression levels of fatty acid oxidation genes after GDF15 knockdown (si-NC: n=3; si-GDF15: n=3). HepG2: Human hepatocellular carcinoma cell line; si-GDF15: interfering RNA; si-NC: negative control for interfering RNA. For bar graphs, data represent mean \pm SEM. *, $P < 0.05$; **, $P < 0.01$; ****, $P < 0.0001$; ns, not significant.

weight, abnormal glucose metabolism and lipid metabolism, particularly abnormal liver lipid deposition, were observed in IVF-ET male mice offspring.

Sex-specific phenotypes, such as male offspring exhibiting more severely impaired glucose metabolism, insulin resistance, abnormal pyruvate tolerance, and earlier weight gain than females, were found in our study. This find-

ing indicates that there may be metabolic gender differences in offspring caused by IVF-ET techniques. To date, various metabolic phenotypes of IVF-ET offspring have been reported. Lower birth weight [28] and catch-up growth [15, 29], normal birth weight [17], and higher body weight were observed with IVF-ET offspring. IVF-ET offspring could be more susceptible to impaired glucose metabolism, insulin resistance, and abnormal pyruvate tolerance

Impact of IVF-ET technology on hepatic lipid metabolism of offspring

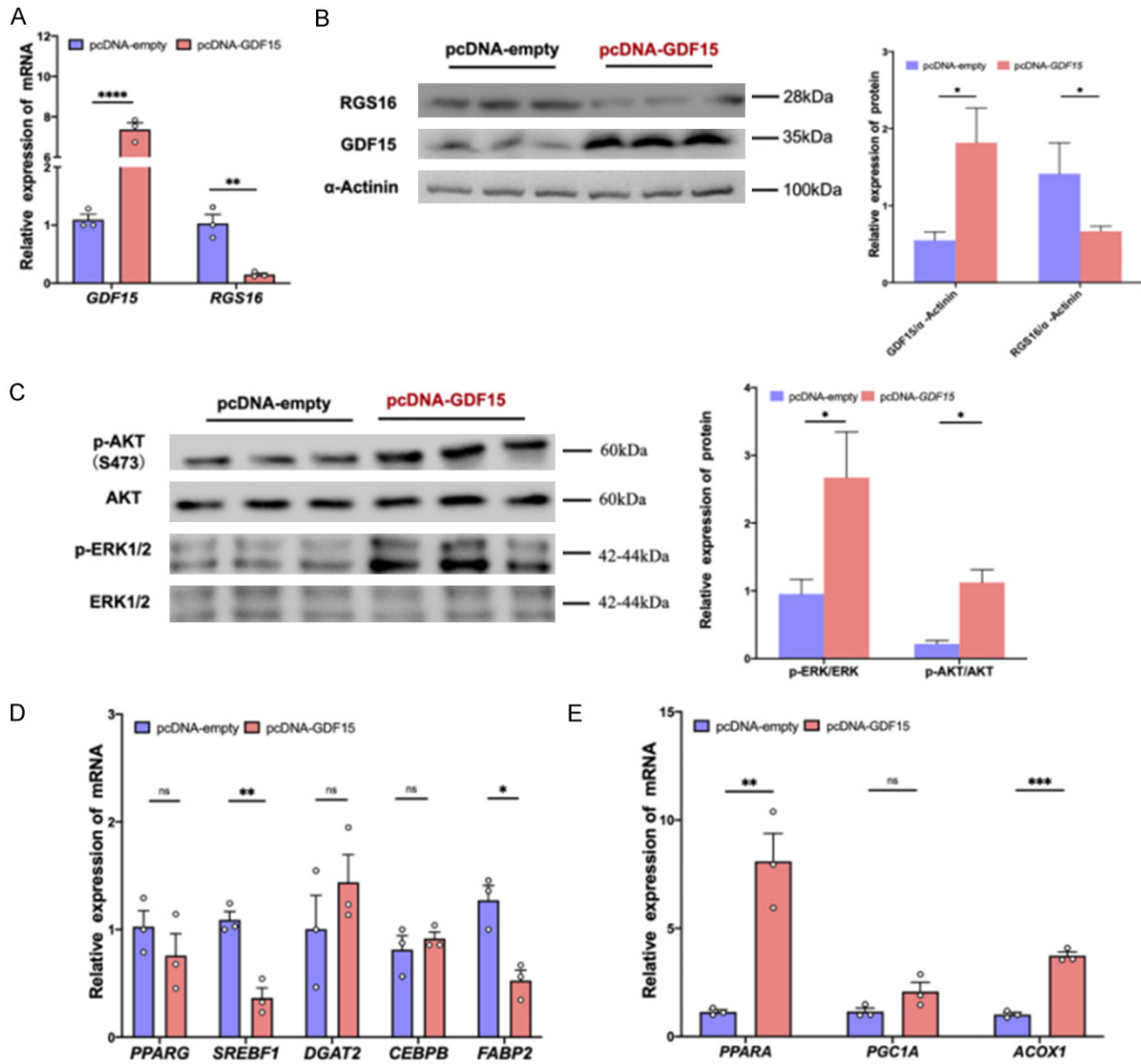


Figure 7. Relationship of GDF15 with lipid metabolism and RGS16. A. mRNA expression levels of GDF15, RGS16 after overexpression of GDF15 (pcDNA-empty: n=3; pcDNA-GDF15: n=3); B. Protein levels of GDF15 and RGS16 after overexpression of GDF15 (pcDNA-empty: n=3; pcDNA-GDF15: n=3); C. Protein levels of AKT, ERK1/2, p-ERK1/2 and p-AKT after overexpression of GDF15 (pcDNA-empty: n=3; pcDNA-GDF15: n=3); D. mRNA expression levels of lipogenic genes after overexpression of GDF15 (pcDNA-empty: n=3-6; pcDNA-GDF15: n=3-6); E. mRNA expression levels of fatty acid oxidation genes after overexpression of GDF15 (pcDNA-empty: n=3-6; pcDNA-GDF15: n=3-6). pcDNA-GDF15: GDF15 Overexpression Plasmid; pcDNA-empty: Empty Plasmid (negative control). For bar graphs, data represent mean \pm SEM. *, $P < 0.05$; **, $P < 0.01$; ***, $P < 0.001$; ****, $P < 0.0001$; ns, not significant.

after receiving a high-fat diet [20]. Severe glucose metabolism dysfunction sometimes occurs only in female offspring and sometimes only in male offspring [15, 16, 18, 29]. The underlying mechanisms of sex-related differences in IVF-ET offspring remain to be fully determined. We presumed that the sex-specific phenotypes might be caused by different mouse strains, culture media, and breeding conditions [17]. In addition, estrogen has a protective effect on glucose metabolism and lipid

metabolism [30]. In vitro manipulation may also affect susceptibility to long-term metabolic disease by affecting genomic imprinting [31], and whether it has gender-specific effects remains to be determined in future studies.

Moreover, we found increased body fat and liver weight, abnormal liver steatosis and lipid deposition, higher TG/LDL-C, and lower HDL-C in the male IVF-ET offspring at 20 weeks. These findings suggest abnormal lipid metabolism in

Impact of IVF-ET technology on hepatic lipid metabolism of offspring

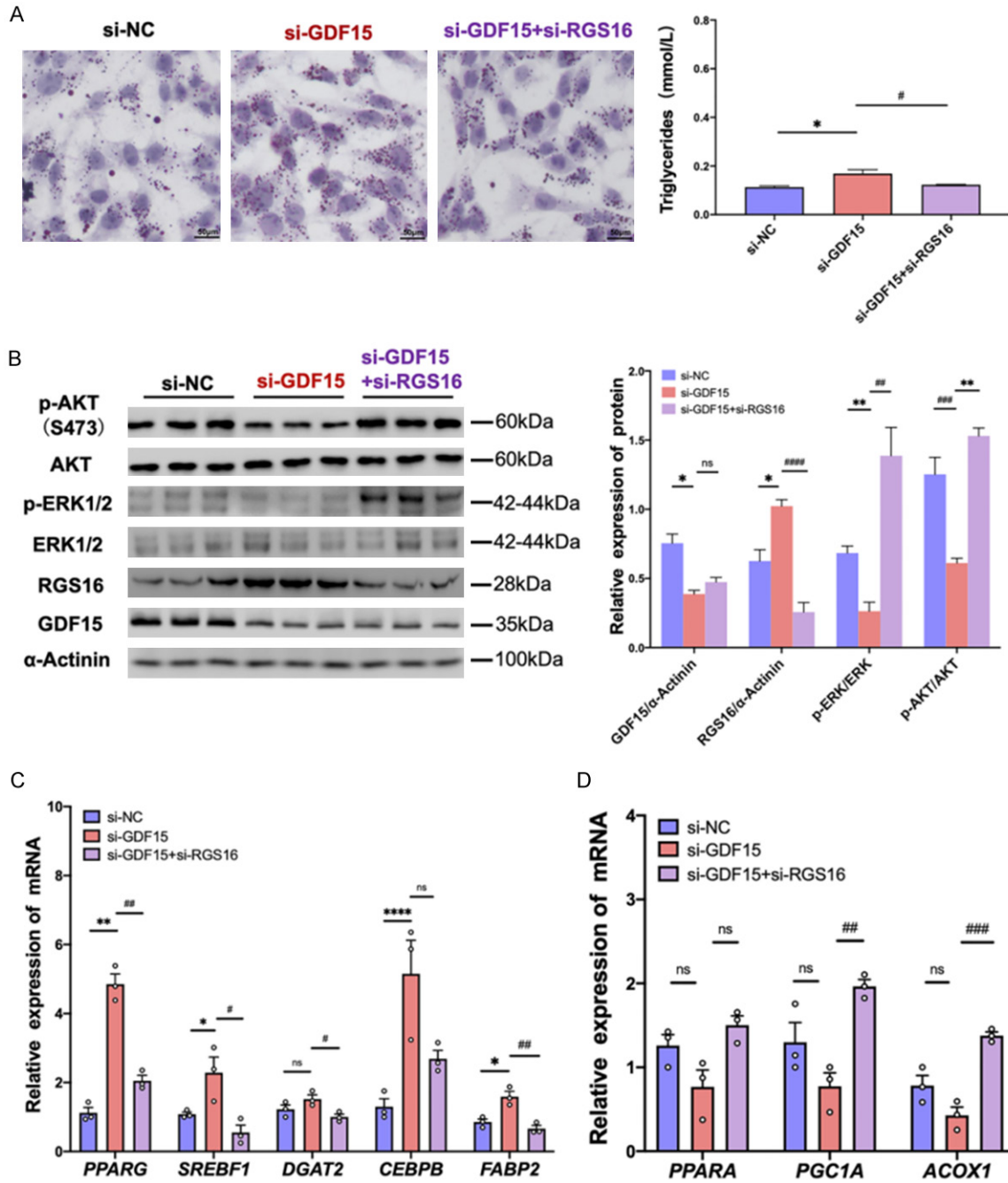


Figure 8. Effect of simultaneous knockdown of GDF15 and RGS16 on lipid metabolism. A. Oil-red O staining in HepG2 cells (scale bar =50 μ m). B. Protein levels of ERK1/2, AKT, p-ERK1/2, p-AKT, GDF15 and RGS16 in si-NC, si-GDF15 and si-GDF15+si-RGS16 (si-NC: n=3; si-GDF15: n=3; si-GDF15+si-RGS16: n=3). C. mRNA expression levels of lipogenic genes of si-NC, si-GDF15 and si-GDF15+si-RGS16 (si-NC: n=3; si-GDF15: n=3; si-GDF15+si-RGS16: n=3); D. mRNA expression levels of fatty acid oxidation genes of si-NC, si-GDF15 and si-GDF15+si-RGS16 (si-NC: n=3; si-GDF15: n=3; si-GDF15+si-RGS16: n=3). Data represent mean \pm SEM. si-NC vs si-GDF15: *, $P < 0.05$; **, $P < 0.01$; ****, $P < 0.0001$; ns, not significant. si-GDF15 vs si-GDF15+si-RGS16: #, $P < 0.05$; ##, $P < 0.01$; ###, $P < 0.001$; ####, $P < 0.0001$; ns, not significant.

IVF-ET male mice. It is well-known that hepatic lipid metabolism plays a key role with essential functions in the de novo synthesis of fatty

acids and ketogenesis [32]. Therefore, we sequenced the liver transcriptome and carried out an in-depth study of the possible mecha-

Impact of IVF-ET technology on hepatic lipid metabolism of offspring

nisms underlying the abnormalities in lipid metabolism. GO, and KEGG enrichment analysis results revealed an upregulated transcriptional status of genes involved in the primary synthesis of hepatic lipids in the livers of IVF-ET mice compared to CON mice. This suggests that the mechanism of increased hepatic lipid deposition in IVF-ET male offspring may be related to abnormal lipid synthesis. Insulin resistance, hyperglycemia, hypertriglyceridemia, and abnormal fatty deposits in the liver are the main features of Non-alcoholic fatty liver disease (NAFLD). Therefore, we speculate that male mice born via IVF-ET might be susceptible to metabolic disorders relative to NAFLD.

It has been shown that increased phosphorylation of the insulin receptors AKT and ERK1/2 contributes to the regulation of hepatic energy metabolism [33-36]. Growth differentiation factor 15 (GDF15), a member of the transforming growth factor- β superfamily, is abundantly expressed in placental trophoblast cells during gestation and is synthesized and secreted mainly in the liver, where it is involved in various biological processes including energy balance, body weight regulation, and cachexia due to cancer and chronic diseases [37, 38]. It can promote fatty acid oxidation and inhibit lipid de novo synthesis in hepatocytes by binding to the GFRAL-RET receptor on the surface of target cells, leading to activation of the downstream AKT and ERK1/2 pathways [39]. Some studies showed that decreased GDF15 in the physiological range can cause increased body weight and fat levels in mice [40]. G protein signaling regulator 16 (RGS16) is expressed in tissues such as the heart, liver, blood-forming cells and brain [41, 42]. High expression of RGS16 leads to hepatic steatosis, reduced blood glucose and β -ketone levels, and decreased gene expression for fatty acid oxidation in the liver; In contrast, *Rgs16* KO mice exhibited the opposite phenotype as increased expression of fatty acid oxidation genes in the liver and increased hepatic fatty acid oxidation rates [26, 43]. In IVF-ET mice, we found downregulation of GDF15, p-ERK1/2, p-AKT, and increased RGS16 and other lipogenic genes in the livers of IVF-ET male offspring. We, therefore, deduced that abnormal lipid metabolism in IVF-ET male offspring might be associated with an abnormal GDF15-RGS16-p-ERK1/2/p-AKT pathway. Combining the known opposite func-

tions reported with GDF15/RGS16 and the opposite expression found in our studies, we presumed that there might be a negative relationship between these two genes. However, no studies have shown an association between GDF15 and RGS16 to date.

In vitro in HepG2 cells, knockdown of GDF15 resulted in abnormal upregulated expression of RGS16, inhibition of the phosphorylation of ERK1/2 and AKT, elevated expression of lipogenic genes, decreased expression of fatty acid oxidation genes, and increased cellular lipid deposition. Overexpression of GDF15 reduced the expression of RGS16, and subsequently increased the phosphorylation of ERK1/2 and AKT, reduced the expression of lipogenic genes, and increased the expression of fatty acid oxidation genes. These findings suggest that there may be a negative regulation between GDF15 and RGS16. Therefore, we speculate that RGS16 downregulated by GDF15 could be a possible mechanism for the abnormal lipid metabolism phenotype in IVF-ET male mice and may be an effective way to improve the metabolic abnormalities in IVF-ET offspring. Nevertheless, this is an in vitro cell experiment and might not fully explain the lipid metabolism pathway of IVF-ET offspring.

However, the factors resulting in reduced hepatic GDF15 expression in IVF-ET offspring remain to be investigated, and epigenetic changes or intergenerational inheritance may be a valid explanation [44, 45]. When genome-wide epigenetic reprogramming occurs, the fertilization and pre-implantation stages are critical periods of development. Manipulations during in vitro culture of fertilized eggs may lead to oxidative stress in fertilized egg cells, affecting cell division [46]. ROS produced by oxidative stress has been shown to regulate epigenetic processes, such as DNA methylation and histone acetylation [47]. The abnormal epigenetic modifications may also be associated with direct, intergenerational, and transgenerational effects in offspring [48].

In summary, the IVF-ET model in this study eliminates the genetic diversity and complex environmental factors in humans and can be used to demonstrate that IVF-ET could have long-term effects on growth and glucolipid metabolism in offspring. Inhibiting RGS16 expression

Impact of IVF-ET technology on hepatic lipid metabolism of offspring

can reverse the abnormal lipid metabolism caused by GDF15 down-regulation, which may be an effective way to alleviate abnormal lipid metabolism in male IVF-ET offspring. However, our findings could not directly represent humans owing to the complex genetic background, the hormonal environment in the body and the use of various drugs in humans. Still, it would provide valuable information for prevention and clinical decision-making.

Conclusion

Male mice born by IVF-ET exhibit a higher risk of glucolipid metabolism manifested as increased body weight, abnormal GTT, ITT, PTT, and abnormal liver lipid deposition. GDF15-RGS16-p-ERK1/2/p-AKT may be the underlying mechanism for lipid metabolism. Realizing the health problems of ART offspring in the long term will help improve the IVF-ET technique to reduce unnecessary adverse effects. This is only one step in that direction and further work is still required.

Acknowledgements

This work was supported by National Key R&D Program of China (2019YFA0802600); National Natural Science Foundation of China (81974244, 81570960); Jiangsu Province's Key Discipline of Prenatal Diagnosis (FXK-201746).

Disclosure of conflict of interest

None.

Address correspondence to: Miao Sun and Bin Wang, Institute for Fetology, The First Affiliated Hospital of Soochow University, Suzhou 215006, Jiangsu, China. E-mail: miaosunsuda@163.com (MS); binwang2233@suda.edu.cn (BW); Min Li, Department of Obstetrics and Gynecology, The First Affiliated Hospital of Soochow University, Suzhou 215006, Jiangsu, China. E-mail: miaoshou181@sina.com

References

- [1] Bai F, Wang DY, Fan YJ, Qiu J, Wang L, Dai Y and Song L. Assisted reproductive technology service availability, efficacy and safety in mainland China: 2016. *Hum Reprod* 2020; 35: 446-452.
- [2] Pourakbari R, Ahmadi H, Yousefi M and Aghebati-Maleki L. Cell therapy in female infertility-

related diseases: emphasis on recurrent miscarriage and repeated implantation failure. *Life Sci* 2020; 258: 118181.

- [3] Tarín JJ, García-Pérez MA and Cano A. Assisted reproductive technology results: why are live-birth percentages so low? *Mol Reprod Dev* 2014; 81: 568-583.
- [4] Fleming TP, Velazquez MA and Eckert JJ. Embryos, DOHaD and David Barker. *J Dev Orig Health Dis* 2015; 6: 377-383.
- [5] Duranthon V and Chavatte-Palmer P. Long term effects of ART: what do animals tell us? *Mol Reprod Dev* 2018; 85: 348-368.
- [6] Basatemur E and Sutcliffe A. Follow-up of children born after ART. *Placenta* 2008; 29 Suppl B: 135-140.
- [7] Chen M, Norman RJ and Heilbronn LK. Does in vitro fertilisation increase type 2 diabetes and cardiovascular risk? *Curr Diabetes Rev* 2011; 7: 426-432.
- [8] Ceelen M, van Weissenbruch MM, Vermeiden JP, van Leeuwen FE and Delemarre-van de Waal HA. Cardiometabolic differences in children born after in vitro fertilization: follow-up study. *J Clin Endocrinol Metab* 2008; 93: 1682-1688.
- [9] Scherrer U, Rimoldi SF, Rexhaj E, Stuber T, Duplain H, Garcin S, de Marchi SF, Nicod P, Germond M, Allemann Y and Sartori C. Systemic and pulmonary vascular dysfunction in children conceived by assisted reproductive technologies. *Circulation* 2012; 125: 1890-1896.
- [10] Sakka SD, Loutradis D, Kanaka-Gantenbein C, Margeli A, Papastamataki M, Papassotiropoulos I and Chrousos GP. Absence of insulin resistance and low-grade inflammation despite early metabolic syndrome manifestations in children born after in vitro fertilization. *Fertil Steril* 2010; 94: 1693-1699.
- [11] Järvisalo MJ, Jartti L, Näntö-Salonen K, Irjala K, Rönnemaa T, Hartiala JJ, Celermajer DS and Raitakari OT. Increased aortic intima-media thickness: a marker of preclinical atherosclerosis in high-risk children. *Circulation* 2001; 104: 2943-2947.
- [12] Rexhaj E, Paoloni-Giacobino A, Rimoldi SF, Fuster DG, Anderegg M, Somm E, Bouillet E, Allemann Y, Sartori C and Scherrer U. Mice generated by in vitro fertilization exhibit vascular dysfunction and shortened life span. *J Clin Invest* 2013; 123: 5052-5060.
- [13] Shi Y, Liu J, Zhu D, Lu L, Zhang M, Li W, Zeng H, Yu X, Guo J, Zhang Y, Zhou X, Gao Q, Xia F, Chen Y, Li M and Sun M. Methylation-reprogrammed CHRM3 results in vascular dysfunction in the human umbilical vein following IVF-ET†. *Biol Reprod* 2022; 106: 687-698.
- [14] Zhang M, Lu L, Zhang Y, Li X, Fan X, Chen X, Tang J, Han B, Li M, Tao J, Gao Q, Xu Z and Sun M. Methylation-reprogrammed AGTR1 results

Impact of IVF-ET technology on hepatic lipid metabolism of offspring

- in increased vasoconstriction by angiotensin II in human umbilical cord vessel following in vitro fertilization-embryo transfer. *Life Sci* 2019; 234: 116792.
- [15] Feuer SK, Liu X, Donjacour A, Lin W, Simbulan RK, Giritharan G, Piane LD, Kolahi K, Ameri K, Maltepe E and Rinaudo PF. Use of a mouse in vitro fertilization model to understand the developmental origins of health and disease hypothesis. *Endocrinology* 2014; 155: 1956-1969.
- [16] Scott KA, Yamazaki Y, Yamamoto M, Lin Y, Melhorn SJ, Krause EG, Woods SC, Yanagimachi R, Sakai RR and Tamashiro KL. Glucose parameters are altered in mouse offspring produced by assisted reproductive technologies and somatic cell nuclear transfer. *Biol Reprod* 2010; 83: 220-227.
- [17] Donjacour A, Liu X, Lin W, Simbulan R and Rinaudo PF. In vitro fertilization affects growth and glucose metabolism in a sex-specific manner in an outbred mouse model. *Biol Reprod* 2014; 90: 80.
- [18] Calle A, Miranda A, Fernandez-Gonzalez R, Pericuesta E, Laguna R and Gutierrez-Adan A. Male mice produced by in vitro culture have reduced fertility and transmit organomegaly and glucose intolerance to their male offspring. *Biol Reprod* 2012; 87: 34.
- [19] Qin N, Zhou Z, Zhao W, Zou K, Shi W, Yu C, Liu X, Dong Z, Mao Y, Liu X, Sheng J, Ding G, Wu Y and Huang H. Abnormal glucose metabolism in male mice offspring conceived by in vitro fertilization and frozen-thawed embryo transfer. *Front Cell Dev Biol* 2021; 9: 637781.
- [20] Narapareddy L, Rhon-Calderon EA, Vrooman LA, Baeza J, Nguyen DK, Mesaros C, Lan Y, Garcia BA, Schultz RM and Bartolomei MS. Sex-specific effects of in vitro fertilization on adult metabolic outcomes and hepatic transcriptome and proteome in mouse. *FASEB J* 2021; 35: e21523.
- [21] Wang LY, Le F, Wang N, Li L, Liu XZ, Zheng YM, Lou HY, Xu XR, Chen YL, Zhu XM, Huang HF and Jin F. Alteration of fatty acid metabolism in the liver, adipose tissue, and testis of male mice conceived through assisted reproductive technologies: fatty acid metabolism in ART mice. *Lipids Health Dis* 2013; 12: 5.
- [22] Jones JG. Hepatic glucose and lipid metabolism. *Diabetologia* 2016; 59: 1098-1103.
- [23] Trefts E, Gannon M and Wasserman DH. The liver. *Curr Biol* 2017; 27: R1147-R1151.
- [24] Wang D, Day EA, Townsend LK, Djordjevic D, Jørgensen SB and Steinberg GR. GDF15: emerging biology and therapeutic applications for obesity and cardiometabolic disease. *Nat Rev Endocrinol* 2021; 17: 592-607.
- [25] Kim JM, Kosak JP, Kim JK, Kissling G, Germolec DR, Zeldin DC, Bradbury JA, Baek SJ and Eling TE. NAG-1/GDF15 transgenic mouse has less white adipose tissue and a reduced inflammatory response. *Mediators Inflamm* 2013; 2013: 641851.
- [26] Pashkov V, Huang J, Parameswara VK, Kedzierski W, Kurrasch DM, Tall GG, Esser V, Gerard RD, Uyeda K, Towle HC and Wilkie TM. Regulator of G protein signaling (RGS16) inhibits hepatic fatty acid oxidation in a carbohydrate response element-binding protein (ChREBP)-dependent manner. *J Biol Chem* 2011; 286: 15116-15125.
- [27] Zou K, Ding G and Huang H. Advances in research into gamete and embryo-fetal origins of adult diseases. *Sci China Life Sci* 2019; 62: 360-368.
- [28] Qin J, Liu X, Sheng X, Wang H and Gao S. Assisted reproductive technology and the risk of pregnancy-related complications and adverse pregnancy outcomes in singleton pregnancies: a meta-analysis of cohort studies. *Fertil Steril* 2016; 105: 73-85, e1-6.
- [29] Chen M, Wu L, Zhao J, Wu F, Davies MJ, Wittert GA, Norman RJ, Robker RL and Heilbronn LK. Altered glucose metabolism in mouse and humans conceived by IVF. *Diabetes* 2014; 63: 3189-3198.
- [30] Katzer K, Hill JL, McIver KB and Foster MT. Lipidema and the potential role of estrogen in excessive adipose tissue accumulation. *Int J Mol Sci* 2021; 22: 11720.
- [31] Bartolomei MS and Ferguson-Smith AC. Mammalian genomic imprinting. *Cold Spring Harb Perspect Biol* 2011; 3: a002592.
- [32] Alves-Bezerra M and Cohen DE. Triglyceride metabolism in the liver. *Compr Physiol* 2017; 8: 1-8.
- [33] Zhang M, Pan J and Huang P. Interaction between RAS gene and lipid metabolism in cancer. *Zhejiang Da Xue Xue Bao Yi Xue Ban* 2021; 50: 17-22.
- [34] Wang X, Zeng J, Wang X, Li J, Chen J, Wang N, Zhang M, Feng Y and Guo H. 2,3,5,4'-tetrahydroxystilbene-2-O- β -D-glucoside induces autophagy of liver by activating PI3K/Akt and Erk pathway in prediabetic rats. *BMC Complement Med Ther* 2020; 20: 177.
- [35] Rebollo-Hernanz M, Aguilera Y, Martin-Cabrejas MA and Gonzalez de Mejia E. Phytochemicals from the cocoa shell modulate mitochondrial function, lipid and glucose metabolism in hepatocytes via activation of FGF21/ERK, AKT, and mTOR pathways. *Antioxidants (Basel)* 2022; 11: 136.
- [36] Hagiwara A, Cornu M, Cybulski N, Polak P, Betz C, Trapani F, Terracciano L, Heim MH, Rüegg MA and Hall MN. Hepatic mTORC2 activates glycolysis and lipogenesis through Akt, glucokinase, and SREBP1c. *Cell Metab* 2012; 15: 725-738.

Impact of IVF-ET technology on hepatic lipid metabolism of offspring

- [37] Sheka AC, Adeyi O, Thompson J, Hameed B, Crawford PA and Ikramuddin S. Nonalcoholic steatohepatitis: a review. *JAMA* 2020; 323: 1175-1183.
- [38] Bootcov MR, Bauskin AR, Valenzuela SM, Moore AG, Bansal M, He XY, Zhang HP, Donnellan M, Mahler S, Pryor K, Walsh BJ, Nicholson RC, Fairlie WD, Por SB, Robbins JM and Breit SN. MIC-1, a novel macrophage inhibitory cytokine, is a divergent member of the TGF-beta superfamily. *Proc Natl Acad Sci U S A* 1997; 94: 11514-11519.
- [39] Zhang Z, Xu X, Tian W, Jiang R, Lu Y, Sun Q, Fu R, He Q, Wang J, Liu Y, Yu H and Sun B. ARR1B1 inhibits non-alcoholic steatohepatitis progression by promoting GDF15 maturation. *J Hepatol* 2020; 72: 976-989.
- [40] Tsai VW, Macia L, Johnen H, Kuffner T, Manadhar R, Jørgensen SB, Lee-Ng KK, Zhang HP, Wu L, Marquis CP, Jiang L, Husaini Y, Lin S, Herzog H, Brown DA, Sainsbury A and Breit SN. TGF- β superfamily cytokine MIC-1/GDF15 is a physiological appetite and body weight regulator. *PLoS One* 2013; 8: e55174.
- [41] Patten M, Bünemann J, Thoma B, Krämer E, Thoenes M, Stübe S, Mittmann C and Wieland T. Endotoxin induces desensitization of cardiac endothelin-1 receptor signaling by increased expression of RGS4 and RGS16. *Cardiovasc Res* 2002; 53: 156-164.
- [42] Kim K, Lee J and Ghil S. The regulators of G protein signaling RGS16 and RGS18 inhibit protease-activated receptor 2/Gi/o signaling through distinct interactions with G α in live cells. *FEBS Lett* 2018; 592: 3126-3138.
- [43] Zhang Y, Higgins CB, Fortune HM, Chen P, Stothard AI, Mayer AL, Swarts BM and DeBosch BJ. Hepatic arginase 2 (Arg2) is sufficient to convey the therapeutic metabolic effects of fasting. *Nat Commun* 2019; 10: 1587.
- [44] Lira-Albarrán S, Liu X, Lee SH and Rinaudo P. DNA methylation profile of liver of mice conceived by in vitro fertilization. *J Dev Orig Health Dis* 2022; 13: 358-366.
- [45] Hanna CW, Demond H and Kelsey G. Epigenetic regulation in development: is the mouse a good model for the human? *Hum Reprod Update* 2018; 24: 556-576.
- [46] Wojsiat J, Korczyński J, Borowiecka M and Żbikowska HM. The role of oxidative stress in female infertility and in vitro fertilization. *Postepy Hig Med Dosw (Online)* 2017; 71: 359-366.
- [47] Hayes P and Knaus UG. Balancing reactive oxygen species in the epigenome: NADPH oxidases as target and perpetrator. *Antioxid Redox Signal* 2013; 18: 1937-1945.
- [48] Ben Maamar M, Nilsson EE and Skinner MK. Epigenetic transgenerational inheritance, gametogenesis and germline development†. *Biol Reprod* 2021; 105: 570-592.

Impact of IVF-ET technology on hepatic lipid metabolism of offspring

Supplementary Table 1. Primers used for RT-qPCR

| Primer | Forward primer (5'-3') | Reverse primer (5'-3') |
|---------------------------------------|-------------------------|------------------------|
| Mouse <i>Gdf15</i> NM_011819 | CTGGCAATGCCTGAACAACG | GGTCGGGACTTGTTCTGAG |
| Mouse <i>Rgs16</i> NM_011267 | GACGCGGCTGGGAATCTTT | GGCCCACTCGAATTTGCTAAT |
| Mouse <i>Pparg</i> NM_011146 | GGAAGACCACTCGCATTCCCTT | GTAATCAGCAACCATTGGGTC |
| Mouse <i>Srebf1</i> NM_011480 | TGACCCGGCTATTCCGTGA | CTGGGCTGAGCAATACAGTTC |
| Mouse <i>Dgat2</i> NM_026384 | GCGCTACTCCGAGACTACTT | GGGCCTTATGCCAGGAAACT |
| Mouse <i>Cebpb</i> NM_001287738 | ACACGTGTAAGTGTGAGCCG | GCTCGAAACGGAAAAGGTTTC |
| Mouse <i>Fabp2</i> NM_007980 | GTGGAAAGTAGACCGGAACGA | CCATCCTGTGTGATTGTCAGTT |
| Mouse <i>Ppara</i> NM_011144 | AACATCGAGTGTGCAATATGTGG | CCGAATAGTTCGCCGAAAGAA |
| Mouse <i>Pgc1a</i> NM_008904 | TATGGAGTGACATAGAGTGTGCT | GTCGCTACACCACTTCAATCC |
| Mouse <i>Acox1</i> NM_015729 | TAACTTCCTCACTCGAAGCCA | AGTTCATGACCCATCTCTGTC |
| Mouse <i>18S</i> NM_003278 | CTCAACACGGGAAACCTCAC | CGCTCCACCAACTAAGAACG |
| Human <i>GDF15</i> NM_004864 | GACCCTCAGAGTTGCACTCC | GCCTGGTTAGCAGGTCCTC |
| Human <i>RGS16</i> NM_002928 | AAGAAGATCCGATCAGCTACCA | GTTGACCTCTTTAGGGGCCTC |
| Human <i>PPARG</i> NM_001330615 | AGCCTGCGAAAGCCTTTTGGTG | GGCTTACATTGAGCAACCTG |
| Human <i>SREBF1</i> NM_004176 | ACAGTGACTTCCCTGGCCTAT | GCATGGACGGGTACATCTTCA |
| Human <i>DGAT2</i> NM_032564 | ATTGCTGGCTCATCGCTGT | GGGAAAGTAGTCTCGAAAGTA |
| Human <i>CEBPB</i> NM_005194 | GACTTCAGCCCGTACCTGGAG | CCCGTAGTCGTCGGAGAAGAG |
| Human <i>FABP2</i> NM_000134 | ATGGCGTTTGACAGCACTTG | TCAGTTCGCTGCTAGATTGT |
| Human <i>PPARA</i> NM_005036 | ATGGTGGACACGGAAAGCC | CGATGGATTGCGAAATCTCTT |
| Human <i>PGC1a</i> NM_013261 | TCTGAGTCTGTATGGAGTGACAT | CCAAGTCGTTACATCTAGTTC |
| Human <i>ACOX1</i> NM_004035 | ACTCGCAGCCAGCGTTATG | AGGGTCAGCGATGCCAAAC |
| Human <i>β-Actin</i> | CATGTACGTTGCTATCCAGGC | CTCCTTAATGTCACGCACGA |

Sequences are shown in the 5' to 3' direction.

Impact of IVF-ET technology on hepatic lipid metabolism of offspring

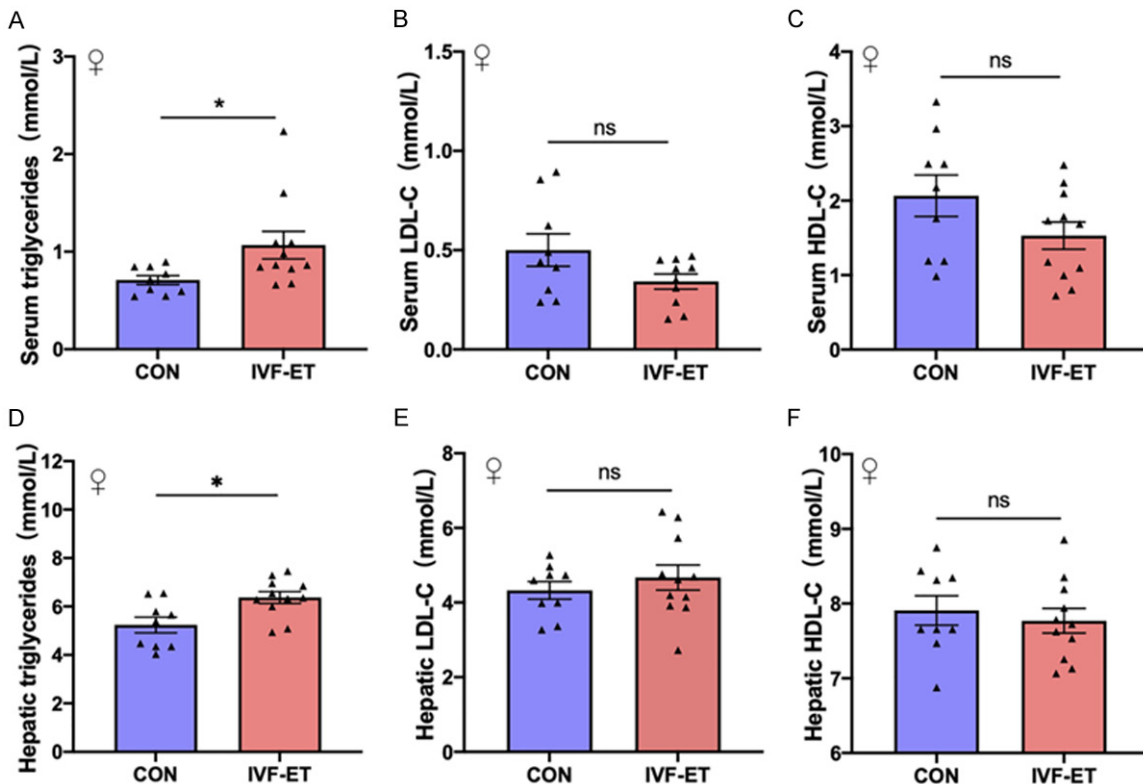
Supplementary Table 2. Antibodies for western blotting

| Primary antibody | | | |
|--|---------------------------|------------|----------|
| 1 st Ab | Company | Cat. No. | Dilution |
| β-actin | Proteintech | 2D4H5 | 1:10000 |
| α-Actinin | Cell Signaling Technology | #6487 | 1:10000 |
| p-ERK1/2 | Cell Signaling Technology | #4370 | 1:1000 |
| ERK1/2 | Cell Signaling Technology | #4695 | 1:1000 |
| p-AKT (Ser473) | Cell Signaling Technology | #4060 | 1:1000 |
| AKT | Cell Signaling Technology | #4691 | 1:1000 |
| GDF15 | Proteintech | 27455-1-AP | 1:1000 |
| GDF15 | Cell Signaling Technology | #8479 | 1:1000 |
| RGS16 | Abcam | ab119424 | 1:1000 |
| Secondary antibody | | | |
| 2 nd Ab | Company | Cat. No. | Dilution |
| HRP-conjugated Affinipure Goat Anti-Mouse IgG (H+L) | Multi Sciences | GAM0072 | 1:10000 |
| HRP-conjugated Affinipure Goat Anti-Rabbit IgG (H+L) | Multi Sciences | GAR0072 | 1:10000 |

Supplementary Table 3. Primers used for siRNA

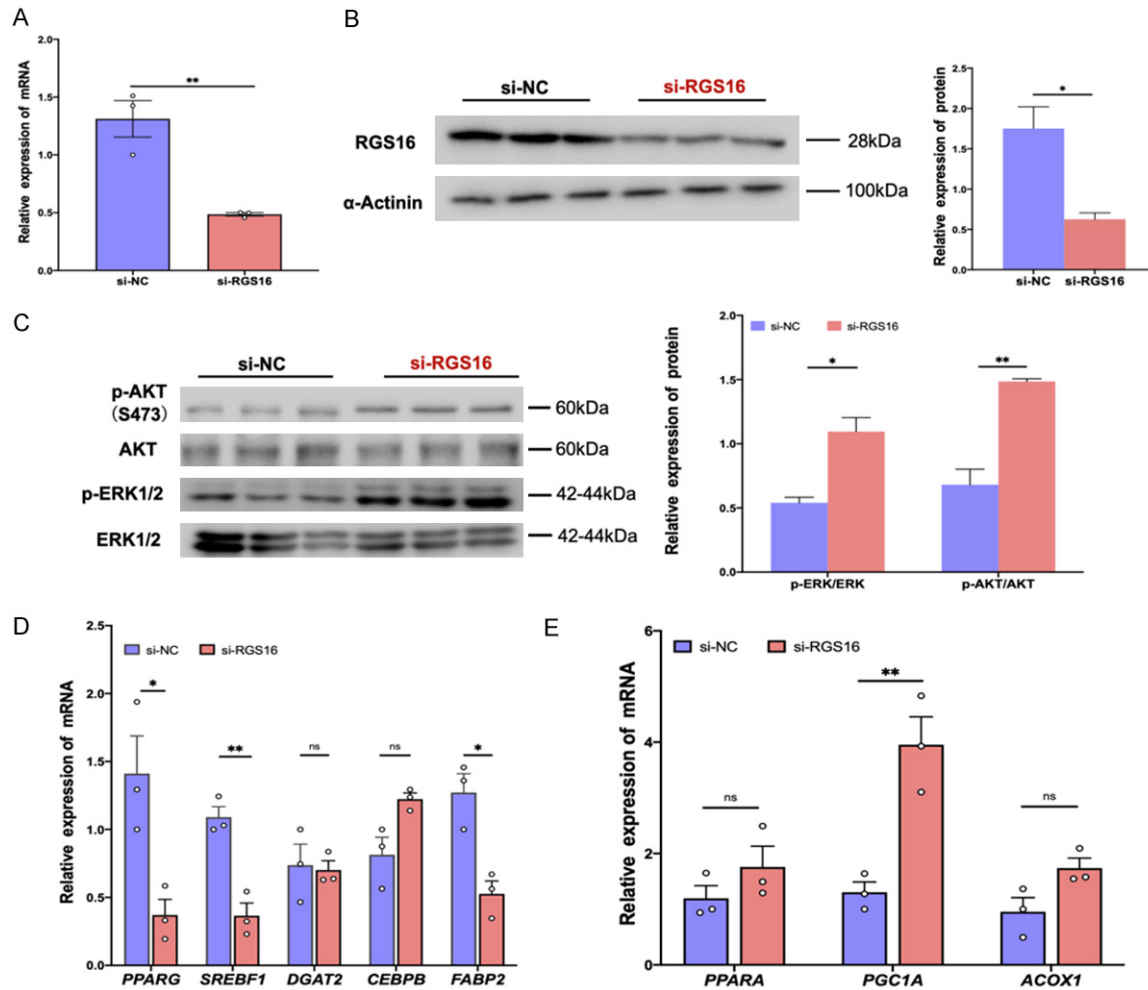
| Primer | Forward oligonucleotide (5'-3') | Reverse oligonucleotide (5'-3') |
|-------------------------------|---------------------------------|---------------------------------|
| <i>GDF15</i> | GCUCCAGACCUAUGAUGACTT | GUCAUCAUAGGUCUGGAGCTT |
| <i>RGS16</i> | GGGCAGUAAACACAGCAAATT | UUUGCUGUGUUUACUGCCCTT |
| Negative control | UUCUCCGAACGUGUCACGUTT | ACGUGACACGUUCGGAGAATT |
| <i>GAPDH</i> Positive control | UGACCUCUACUACAUGGUUTT | AACCAUGUAGUUGAGGUCATT |

Sequences are shown in the 5' to 3' direction.



Impact of IVF-ET technology on hepatic lipid metabolism of offspring

Supplementary Figure 1. Analysis of lipid metabolism factors in female offspring. A-C. Plasma levels of Triglycerides, LDL-C, HDL-C (CON: n=10; IVF-ET: n=11). D-F. Triglycerides, LDL-C, HDL-C levels in liver tissue (CON: n=8; IVF-ET: n=10). TG, Triacylglycerol; HDL-C, High-Density Lipoprotein Cholesterol; LDL-C, Low-Density Lipoprotein Cholesterol. Data represent mean \pm SEM. *, $P < 0.05$; ns, not significant.



Supplementary Figure 2. Role of RGS16 in lipid metabolism. RGS16 knockdown (KD) in HepG2 cells evaluated by (A) mRNA or (B) protein levels; (C) Protein expression of ERK1/2, AKT, p-ERK1/2, or p-AKT after RGS16 knockdown (si-NC: n=3-4; si-RGS16: n=3-4). (D) mRNA expression levels of lipogenic genes after RGS16 knockdown (si-NC: n=3; si-RGS16: n=3); (E) mRNA expression levels of fatty acid oxidation genes after RGS16 knockdown (si-NC: n=3; si-RGS16: n=3). All data are expressed as mean \pm SEM. *, $P < 0.05$; **, $P < 0.01$; ns, not significant. Relative to negative control, by two-tailed Student's t-test.